

Measurements of the energy spectrum of electrons emanating from solid materials irradiated by a picosecond laser

C. A. Di Stefano, C. C. Kuranz, J. F. Seely, A. G. R. Thomas, R. P. Drake, P. A. Keiter, G. J. Williams, J. Park, H. Chen, M. J. MacDonald, A. M. Rasmus, W. C. Wan, N. R. Pereira, A. S. Joglekar, A. McKelvey, Z. Zhao, S. R. Klein, G. E. Kemp, L. C. Jarrott, C. M. Krauland, J. Peebles, and B. Westover

Citation: *Physics of Plasmas* **22**, 043113 (2015); doi: 10.1063/1.4917325

View online: <http://dx.doi.org/10.1063/1.4917325>

View Table of Contents: <http://scitation.aip.org/content/aip/journal/pop/22/4?ver=pdfcov>

Published by the **AIP Publishing**

Articles you may be interested in

[Directed fast electron beams in ultraintense picosecond laser irradiated solid targets](#)

Appl. Phys. Lett. **107**, 091111 (2015); 10.1063/1.4930074

[Modeling target bulk heating resulting from ultra-intense short pulse laser irradiation of solid density targets](#)

Phys. Plasmas **20**, 123116 (2013); 10.1063/1.4833618

[Strong terahertz radiation from relativistic laser interaction with solid density plasmas](#)

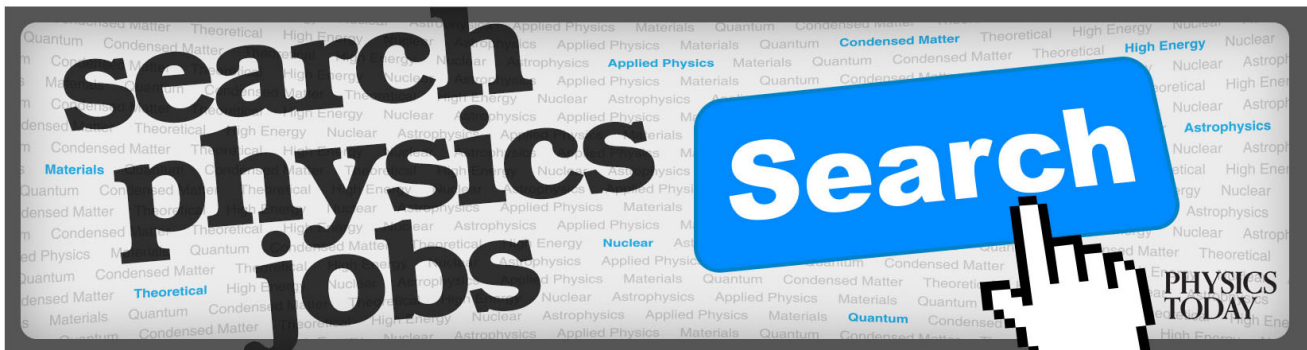
Appl. Phys. Lett. **100**, 254101 (2012); 10.1063/1.4729874

[Effects of target charging and ion emission on the energy spectrum of emitted electrons](#)

Phys. Plasmas **18**, 053107 (2011); 10.1063/1.3587123

[Measurement of preheat due to fast electrons in laser implosions of cryogenic deuterium targets](#)

Phys. Plasmas **12**, 062703 (2005); 10.1063/1.1928193



Measurements of the energy spectrum of electrons emanating from solid materials irradiated by a picosecond laser

C. A. Di Stefano,^{1,a)} C. C. Kuranz,¹ J. F. Seely,² A. G. R. Thomas,¹ R. P. Drake,¹ P. A. Keiter,¹ G. J. Williams,³ J. Park,³ H. Chen,³ M. J. MacDonald,^{1,4} A. M. Rasmus,¹ W. C. Wan,¹ N. R. Pereira,⁵ A. S. Joglekar,¹ A. McKelvey,¹ Z. Zhao,¹ S. R. Klein,¹ G. E. Kemp,³ L. C. Jarrott,⁶ C. M. Krauland,^{1,6} J. Peebles,⁶ and B. Westover⁶

¹University of Michigan, Ann Arbor, Michigan 48109, USA

²Artep, Inc., Ellicott City, Maryland 21042, USA

³Lawrence Livermore National Laboratory, Livermore, California 94551, USA

⁴SLAC National Accelerator Laboratory, Menlo Park, California 94025, USA

⁵Ecopulse, Inc., Springfield, Virginia 22150, USA

⁶University of California, San Diego, Energy Research Center, La Jolla, California 92093, USA

(Received 10 November 2014; accepted 30 March 2015; published online 13 April 2015)

In this work, we present the results of experiments observing the properties of the electron stream generated laterally when a laser irradiates a metal. We find that the directionality of the electrons is dependent upon their energies, with the higher-energy tail of the spectrum (~ 1 MeV and higher) being more narrowly focused. This behavior is likely due to the coupling of the electrons to the electric field of the laser. The experiments are performed by using the Titan laser to irradiate a metal wire, creating the electron stream of interest. These electrons propagate to nearby spectator wires of differing metals, causing them to fluoresce at their characteristic *K*-shell energies. This fluorescence is recorded by a crystal spectrometer. By varying the distances between the wires, we are able to probe the divergence of the electron stream, while by varying the medium through which the electrons propagate (and hence the energy-dependence of electron attenuation), we are able to probe the energy spectrum of the stream. © 2015 AIP Publishing LLC.

[<http://dx.doi.org/10.1063/1.4917325>]

I. INTRODUCTION

During the complex interaction between a laser pulse and an irradiated material, a variety of physical processes can contribute to the production of a stream of high-energy electrons, especially when the laser irradiance becomes sufficiently high. For example, the ponderomotive force due to the electromagnetic field of the laser can drive a significant electrostatic field, which in turn will accelerate electrons.^{1,2} Electrons can also acquire energy via vacuum heating, in which an escaping electron is pulled back into the plasma generated by the laser irradiation,^{3,4} via resonance absorption, in which the electric-field oscillations of the laser excite plasma waves,^{5,6} or by interaction with the standing-wave pattern arising when reflected laser light interacts with the incident pulse.⁷ Other circumstances of the laser irradiation event, such as boring of the laser into the material, can lead to increased electron acceleration compared with the nominal interaction of the laser with a flat surface.^{8–10}

Under certain conditions, these processes can lead to a significant fraction of the laser energy, up to several tens of percent, being converted into the kinetic energy of these electrons,^{11,12} and with modern laser technology, the characteristic energies of typical streams can be MeV or larger.^{13–15} Such an electron stream can have a considerable effect on nearby materials. This can either be a useful feature, for

example, as a possible method to significantly increase fusion fuel heating in the fast-ignition concept^{11,15–18} or it can be a complicating factor in experiments involving a laser drive, where, for example, hot-electron heating can alter precisely chosen initial conditions¹⁹ or introduce noise signal in imaging diagnostics,^{20,21} thereby degrading data quality. The exact behavior of the previously-described phenomena remains challenging to understand due to the complexity of the physics involved,¹⁷ and the present experiments are designed to provide a measurement of the energy spectrum of an electron stream produced in this manner.

One method of doing so is to position a second material such that it intercepts the electron stream. Interactions between the electrons and this spectator material cause the latter material to fluoresce at its characteristic *K*-shell energies, and this fluorescence can be measured with a spectrometer. This technique has the advantage that a spectator sample can often be positioned much more easily and precisely than a diagnostic instrument. Previous results employing this technique suggest that the oscillating electric field of the laser tends to couple to the electrons in the material, accelerating the electrons preferentially along the direction of the field,¹³ and resulting in characteristic energies of roughly MeV order.^{13,22}

In the present experiments, we seek a more detailed understanding of the energy spectrum of the electron stream coupled to the electric field of the laser. Because a fluorescence event on its own only indicates that an electron has

^{a)}Author to whom correspondence should be addressed. Electronic mail: carlosds@umich.edu

arrived at the spectator material, we use varying geometric arrangements to learn more about the directionality and spectral content of the electron stream. For example, divergence of the electrons as they propagate will result in reduced fluorescence as the spectator wire is placed farther from the source. Forcing the electrons to propagate through different media results in attenuation that is dependent upon the energy of the electrons and the properties of these media. The resulting variations in detected fluorescence constrain the possible properties of the electron stream causing the emission.

II. EXPERIMENTAL CONDITIONS

The main experimental system, shown in Fig. 1, consists of three elemental metal wires, 0.5 mm in diameter and 3 mm long, mounted onto a substrate. The axes of these wires are oriented horizontally, parallel to the y direction in Figs. 1(b) and 1(c). The three wires are also coplanar with each other and the vertical direction, corresponding to the y - z plane in Figs. 1(b) and 1(c). They are organized in this manner because the irradiating laser beam is polarized vertically, corresponding to the z direction in Figs. 1(b) and 1(c). The result is that the upper and lower (spectator) wires lie along the polarization direction relative to the center (irradiated) wire. The substrate was designed such that the center wire is embedded upon its surface, pressed into a channel of depth 0.25 mm, such that approximately half the wire protrudes above the substrate surface. Meanwhile, the lower

wire is completely encased by substrate material, and the upper wire is suspended from two struts. The idea is that the direct path between the irradiated and suspended wires traverses vacuum, and the direct path between the irradiated and buried wires traverses substrate material. In some cases, the substrate is made of Teflon, and in others it is made of aluminum. These two materials represent extremes of high and low resistivity, respectively, and were chosen to help isolate resistive effects on the electron propagation.¹³ The outer-edge-to-outer-edge spacing of the wires is also varied, being 0.5 mm in some cases and 1.0 mm in others. The experiments are conducted using silver as the suspended wire and tin as the buried wire.

The hafnium wire is irradiated by a single Titan 1053-nm laser pulse, nominally at an energy of 100 J and of 1 ps duration, focused to a nominally 10- μ m-diameter spot. The interaction of the laser with the hafnium generates a stream of electrons, some of which propagate towards the silver and tin wires, in turn causing these wires to emit X rays at their characteristic $K\alpha$ and $K\beta$ energies. These two materials were chosen for resolvability of their K lines by the diagnosing X-ray spectrometer, while their relatively low Z permits stronger K -line emission due to the larger cross-section for K -shell ionization.²³

III. EXPERIMENTAL RESULTS

The primary diagnostic was the Lawrence-Livermore Crystal Spectrometer (LLCS),²⁴ a transmission crystal spectrometer employing a cylindrically-curved (10–11) quartz crystal with a 254-mm radius of curvature in a Cauchois^{25,26} geometrical configuration, producing spectral images upon an imaging plate located on the Rowland circle. Fig. 2(a) shows an example of a raw data image obtained by LLCS. The crystal only disperses in the horizontal direction such that, if the photon source is isotropic, the line should be uniform in the vertical direction. This enables the signal to be averaged over the length of the line, which results in an accurate measurement. Random noise fluctuations are small in magnitude as well as small in spatial scale compared to the width of the broadened spectral line.^{26,27} These noise fluctuations therefore create an error of only a few percent in the overall line signal. Finally, the resulting signal can be calibrated to actual photon counts per pixel on the detector, by accounting for the sensitivity of the imaging plate as well as the response of the scanner to the recorded signal.^{28,29}

Fig. 2(b) shows the result of this method for the data in Fig. 2(a). Although there is significant background signal present, the large-scale structure of the background is very consistent, permitting it to be easily removed, and small-scale noise fluctuations are small, as described above. Typical measurement uncertainties, found by fitting second-order polynomials to various sections of the curve in Fig. 2(b), are roughly 1% for the brightest lines and roughly 5%–8% for the faintest lines. It turns out, as will be discussed further in Sec. IV, that uncertainty introduced by normal shot-to-shot variations in observed signal is much more important than that introduced by the measurement.

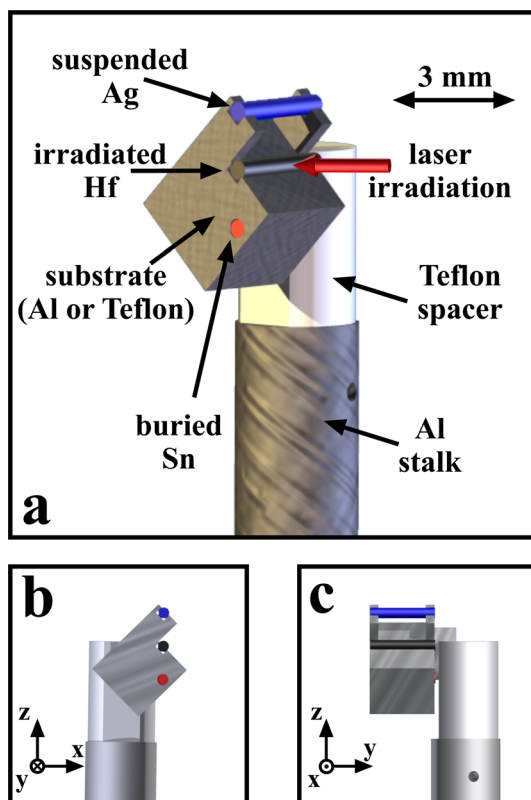


FIG. 1. (a) Geometrical configuration of the experimental system. The direction of polarization of the laser corresponds to the direction labeled z in frames (b) and (c).

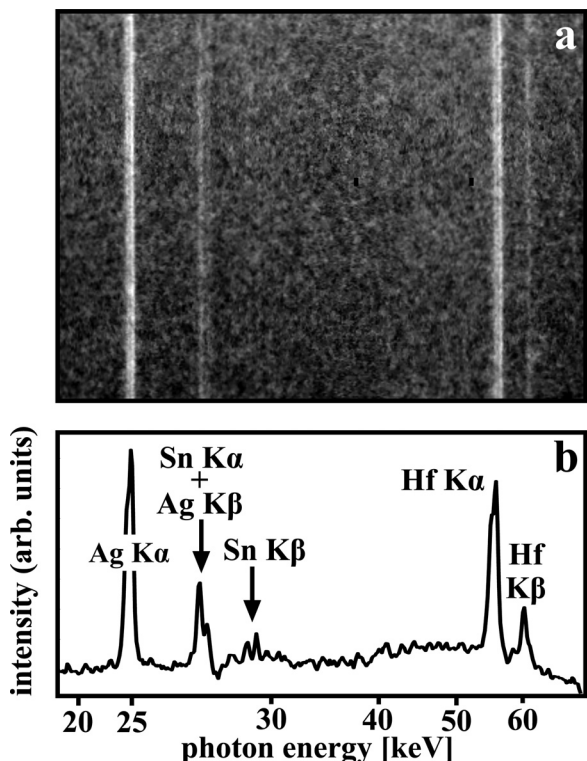


FIG. 2. (a) Raw data image. Because the spectral lines are nominally uniform in the vertical direction on the imaging plate, it is possible, for most observable lines, to obtain a robust measurement. (b) Horizontal line sample of the data in frame (a). The sample was averaged over a vertical region of 400 pixels, corresponding to 2 cm on the imaging plate. The K-shell emission lines are clearly discernible for all three wire materials, except for the Ag K β lines, which happen to be superposed upon the Sn K α ones.

Finally, the LLCS diagnostic also records a pinhole image of the fluorescing experimental system. These images are useful for identifying what parts of the system are fluorescing. This in turn provides insight into the propagation path of electrons through the system. An example of these pinhole images is shown in Fig. 3(a). A rendering of the view of the pinhole is shown in Fig. 3(b) for reference. In Fig. 3(a), a hot spot, visible at the center of the image, corresponds to the location of irradiation of the Hf wire. Emission from the spectator wires is also present as well as

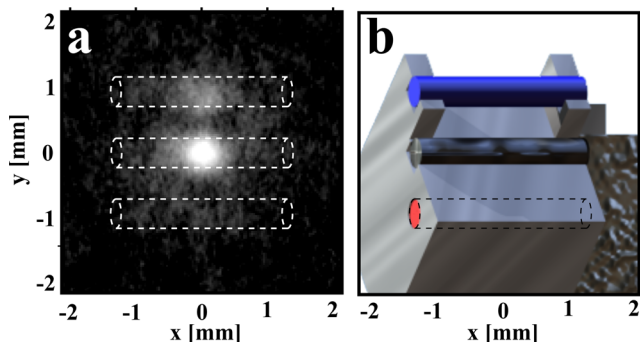


FIG. 3. Pinhole image captured by the LLCS diagnostic. The image, foreshortened about 8% in the horizontal direction due to the angle of view of LLCS, shows the irradiation spot at its center, a hot spot at the center of the suspended wire directly above it, and weaker emission along the full lengths of all three wires.

weak emission from the body of the substrate. Although emission from the entire length of the spectator wires is visible, it is noticeably stronger near the center of the suspended wire, directly above the irradiated wire. The buried wire behaves similarly, although the overall signal is weaker. These general characteristics are consistent across data from all iterations of the experiment.

The measured K α_1 + K α_2 emissions for all iterations of the experiment are shown in Fig. 4. Signal from the suspended wires is plotted as black points, while signal from the buried wires is plotted as red points. The substrate material is indicated by the fill color of the data point: white for Teflon and gray for aluminum. Each configuration was repeated 5 times, and the plotted points are the means of the measurements within each configuration. The error bars shown correspond to the standard deviation of these means. The two configurations at each individual wire spacing are slightly offset from the 0.5 and 1.0 mm locations along the abscissa for readability. Variation in the reproducibility of the irradiation conditions is discussed in the Appendix.

The system was also diagnosed using three Electron Positron Proton Spectrometers (EPPS),³⁰ located in the horizontal plane at angles of 60°, 140°, and 180° to the direction of incidence of the laser. The EPPS diagnostic employs permanent magnets to deflect incoming charged particles at angles that vary according to their energies and then records the altered positions of the particles on imaging plates. Confidence in the source of electrons arriving at the detector was limited to energies above 2 MeV. Distortions in the signal below 2 MeV indicates that these electrons may not be emanating directly from the laser irradiation event. This could occur, for instance, due to lower-energy electrons propagating through the target or being influenced by strong electromagnetic fields generated on the surface of the system. The three curves in Fig. 5 show an example of the spectra generated by the experiment. These data provide direct evidence of the production of high-energy electrons as well as direct evidence of their directional dependence.

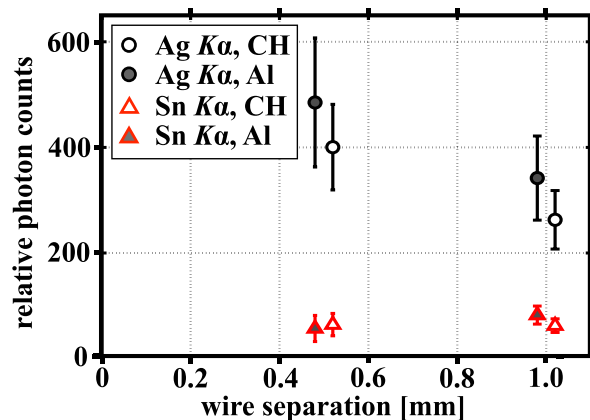


FIG. 4. Secondary fluorescence recorded by LLCS for the four main experimental configurations. The signal from the suspended spectator wires is shown as black circles, while the signal from the buried wires is shown as red triangle. White-filled points indicate Teflon (CF) substrates, while gray-filled points indicate aluminum substrates.

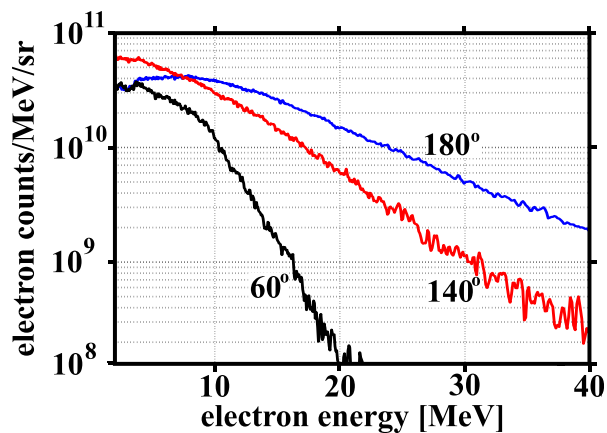


FIG. 5. High-energy (>2 MeV) electron spectra measured by the EPPS diagnostic in the horizontal plane, measured at various angles from the direction of incidence of the laser.

IV. DISCUSSION

Based on purely geometrical consideration, if the electrons were to propagate isotropically away from the irradiated wire, we would expect the X-ray signal from the suspended wire in the 1.0-mm spacing to be roughly half that from the wires in the 0.5-mm spacing. This is because the spectator wire is long in one direction, leading to a $1/r$ scaling for wire separation r . In fact, the variation is much less, roughly a factor of 1.5, as shown in Fig. 4. This suggests that there is some preference for propagation along the laser polarization direction. The brighter emission seen from the part of the spectator wire directly above the laser spot also supports this conclusion.

Meanwhile, electrons propagating towards the buried wire experience the additional effect of attenuation in the substrate. In order for an electron to propagate through 0.5 mm or 1.0 mm of aluminum without being attenuated, it must have a minimum energy of 0.25 or 0.5 MeV, respectively. Monte Carlo simulation of our wire configurations²² indicates that, for a beam of 1-MeV electrons, approximately 80% will scatter away through 0.5 mm of Al, and more than 95% will scatter away through 1.0 mm of Al. The fact that we observe much lower signal from the buried wires and no variation with separation suggests something further about the energy spectrum. First, there is a higher-energy component to the electron energy spectrum that is highly directional, which is likely to propagate through the substrate without being attenuated, and without diverging. Second, there is a lower-energy component that behaves more isotropically, which is less likely to reach the buried wire.

The presence of these two components would explain the fact that many electrons reach the suspended wires, and that this stream diverges as it propagates, but not as much as expected. It would also explain the fact that fewer electrons reach the buried wire, and that this stream does not appear to diverge as it propagates. Finally, this is also consistent with our expectation that electrons propagate away from the source in all directions, but some will couple to the electric field of the laser and be accelerated along the direction of polarization.

V. CONCLUSIONS

The experiments we have presented here provide evidence of the coupling of electrons to the electric field of a laser incident upon a material. The behavior of these electrons as they propagate through various media is dependent both on their initial energy and on their directionality, and we have used this to determine some properties of the electron stream. First, this stream has higher- and lower-energy components, with an overall characteristic energy of roughly 1 MeV. Second, the high-energy component tends to be more strongly directional than the low-energy component. This behavior is consistent with what we would expect from the coupling of the electrons to the electric field of the laser.

Future work, both experimental and computational, is being planned in order to further explore these effects. Experiments designed to isolate the spectral components of the electron stream and examine directional effects would provide more detail regarding the behavior of the electrons. Meanwhile, we are working to develop simulations that model both the generation of the electron stream by the laser as well as the subsequent propagation of the stream through the various materials in the system. Pairing these simulations with our experimental results will help to quantify the effects we observed more precisely, as well as further our understanding of the reliability of existing models of laser/solid interactions.

ACKNOWLEDGMENTS

The authors would like to acknowledge the contributions of Robb Gillespie at the University of Michigan, who machined the substrates, spacers, and stalks used to construct the experiment.

This work was funded by the U.S. Department of Energy, through the NNSA-DS and SC-OFES Joint Program in High-Energy-Density Laboratory Plasmas, Grant No. DE-NA0001840 and by the Defense Threat Reduction Agency, Grant No. DTRA-1-10-0077. The work of authors affiliated with Lawrence Livermore National Laboratory (LLNL) was performed under the auspices of the U.S. Department of Energy by LLNL under Contract No. DE-AC52-07NA27344.

APPENDIX: MEASUREMENT CONSIDERATIONS

Several assumptions have been made about the experimental system in order to produce the experimental results presented in Sec. III. We discuss these here, in turn. First, we consider the convolvement of split lines on the detector, especially the $K\alpha$ doublets and $K\beta$ triplets. This can be seen in Fig. 2(b). It is well-known that spectral lines tend to broaden in a Cauchy-Lorentz profile^{26,27} and that the relative intensities of the lines in a given set are quantum mechanical in nature and should not be affected by the details of our experiment. By assuming a Cauchy-Lorentz profile for each line, we are able to produce a best fit for the peaks in the data by iteratively adjusting the height and wavelength of each line. The result agrees with well-known, tabulated values.³¹ For simplicity, we have therefore chosen to refer to the overall $K\alpha$ and $K\beta$ signals and not to individual lines.

Second, we require a method to separate the convolved Sn $K\alpha$ and Ag $K\beta$ lines in our data. The ratio of $K\alpha$ to $K\beta$ emission by a given material is temperature-dependent, but our wires are sufficiently large that we expect neither the irradiating laser nor the stream of generated electrons to significantly heat them.³² These ratios, for cold materials, are also well-known and tabulated.³¹ In order to confirm that this is the case, we performed a separate experiment, in which we removed the Sn wire and the substrate from the system, leaving only the irradiated wire and a Ag spectator wire. The resulting Ag $K\alpha/K\beta$ value was 5.35, in close agreement with the predicted value of 5.26. We are therefore confident that the emission is cold, and we can deconvolve the Sn $K\alpha$ and Ag $K\beta$ lines.

Third, the validity of our experiment result depends upon the electron stream propagation upwards from the source being equivalent to the stream propagating downwards from the source. In order to confirm this, we performed an experiment in which we removed the substrate from the system, leaving only the three exposed wires attached to the stalk. The expected emission from each material depends on its cross-section for K-shell ionization by incoming electrons as well as the density of atoms within each wire. Previous work^{13,33} has established that the typical energies of the electrons involved here are of roughly MeV order. In this energy range and higher, these cross-sections are approximately independent of electron energy,²³ and we can therefore predict the expected signal ratio, $K_{Ag}/K_{Sn} = 1.85$, for each material under identical electron conditions. The experimental result is 1.83, confirming that an equivalent electron stream propagates towards each spectator wire.

Finally, there was significant jitter both in the delivered laser energy (typical values were roughly between 100J and 120J) and in laser prepulse energy (typical values were roughly between 10 mJ and 70 mJ, with no further information about the prepulse profile available). We examined the relationship between these energies with the signal observed from both the irradiated and spectator wires over approximately 25 iterations of the experiment and found no significant correlations. We therefore believe that the electron streams created are highly variable shot-to-shot and not particularly sensitive to the exact energy profile delivered by the laser.

¹W. L. Kruer and K. Estabrook, *Phys. Fluids* **28**, 430 (1985).

²S. C. Wilks and W. Kruer, *IEEE J. Quantum Electron.* **33**, 1954 (1997).

³F. Brunel, *Phys. Rev. Lett.* **59**, 52 (1987).

⁴P. Gibbon and A. R. Bell, *Phys. Rev. Lett.* **68**, 1535 (1992).

⁵K. Estabrook and W. L. Kruer, *Phys. Rev. Lett.* **40**, 42 (1978).

⁶K. R. Manes, V. C. Rupert, J. M. Auerbach, P. Lee, and J. E. Swain, *Phys. Rev. Lett.* **39**, 281 (1977).

⁷G. E. Kemp, A. Link, Y. Ping, D. W. Schumacher, R. R. Freeman, and P. K. Patel, *Phys. Plasmas* **20**, 033104 (2013).

⁸S. C. Wilks, W. L. Kruer, M. Tabak, and A. B. Langdon, *Phys. Rev. Lett.* **69**, 1383 (1992).

⁹W. L. Kruer and S. C. Wilks, *Plasma Phys. Controlled Fusion* **34**, 2061 (1992).

¹⁰Y. Ping, R. Shepherd, B. F. Lasinski, M. Tabak, H. Chen, H. K. Chung, K. B. Fournier, S. B. Hansen, A. Kemp, D. A. Liedahl, K. Widmann, S. C. Wilks, W. Rozmus, and M. Sherlock, *Phys. Rev. Lett.* **100**, 085004 (2008).

¹¹R. Kodama, P. A. Norreys, K. Mima, A. E. Dangor, R. G. Evans, H. Fujita, Y. Kitagawa, K. Krushelnick, T. Miyakoshi, N. Miyanaga, T. Norimatsu, S. J. Rose, T. Shozaki, K. Shigemori, A. Sunahara, M. Tampo, K. A. Tanaka, Y. Toyama, T. Yamanaka, and M. Zepf, *Nature* **412**, 798–802 (2001).

¹²K. B. Wharton, S. P. Hatchett, S. C. Wilks, M. H. Key, J. D. Moody, V. Yanovsky, A. A. Offenberger, B. A. Hammel, M. D. Perry, and C. Joshi, *Phys. Rev. Lett.* **81**, 822 (1998).

¹³J. F. Seely, C. I. Szabo, P. Audebert, E. Brambrink, E. Tabakhoff, and L. T. Hudson, *Phys. Plasmas* **17**, 023102 (2010).

¹⁴F. N. Beg, A. R. Bell, A. E. Dangor, C. N. Danson, A. P. Fews, M. E. Glinsky, B. A. Hammel, P. Lee, P. A. Norreys, and M. Tatarakis, *Phys. Plasmas* **4**, 447 (1997).

¹⁵J. Myatt, W. Theobald, J. A. Delettrez, C. Stoeckl, M. Storm, T. C. Sangster, A. V. Maximov, and R. W. Short, *Phys. Plasmas* **14**, 056301 (2007).

¹⁶R. Kodama, K. Mima, K. A. Tanaka, Y. Kitagawa, H. Fujita, K. Takahashi, A. Sunahara, K. Fujita, H. Habara, T. Jitsuno, Y. Sentoku, T. Matsushita, T. Miyakoshi, N. Miyanaga, T. Norimatsu, T. Sonomoto, M. Tampo, Y. Toyama, and T. Yamanaka, *Phys. Plasmas* **8**, 2268 (2001).

¹⁷M. H. Key, *Phys. Plasmas* **14**, 055502 (2007).

¹⁸M. Tabak, J. Hammer, M. E. Glinsky, W. L. Kruer, S. C. Wilks, J. Woodworth, E. M. Campbell, M. D. Perry, and R. J. Mason, *Phys. Plasmas* **1**, 1626 (1994).

¹⁹G. Malamud, C. A. Di Stefano, Y. Elbaz, C. M. Huntington, C. C. Kuranz, P. A. Keiter, and R. P. Drake, *High Energy Density Phys.* **9**, 122 (2013).

²⁰C. C. Kuranz, B. E. Blue, R. P. Drake, H. F. Robey, J. F. Hansen, J. P. Knauer, M. J. Grosskopf, C. Krauland, and D. C. Marion, *Rev. Sci. Instrum.* **77**, 10E327 (2006).

²¹C. M. Krauland, L. C. Jarrott, R. P. Drake, P. A. Keiter, C. C. Kuranz, B. Westover, H. Sawada, D. N. Kaczala, and P. Bonfiglio, *Rev. Sci. Instrum.* **83**, 10E528 (2012).

²²J. F. Seely, C. I. Szabo, P. Audebert, and E. Brambrink, *Phys. Plasmas* **18**, 062702 (2011).

²³H. Kolbenstvedt, *J. Appl. Phys.* **38**, 4785 (1967).

²⁴J. F. Seely, C. I. Szabo, P. Audebert, E. Brambrink, E. Tabakhoff, G. E. Holland, L. T. Hudson, A. Henins, P. Indelicato, and A. Gumberidze, *High Energy Density Phys.* **5**, 263 (2009).

²⁵Y. Cauchois, *J. Phys. Radium* **3**, 320 (1932).

²⁶J. F. Seely, L. T. Hudson, G. E. Holland, and A. Henins, *Appl. Opt.* **47**, 2767 (2008).

²⁷J. F. Seely, G. E. Holland, L. T. Hudson, and A. Henins, *Appl. Opt.* **47**, 5753 (2008).

²⁸A. L. Meadowcroft, C. D. Bentley, and E. N. Stott, *Rev. Sci. Instrum.* **79**, 113102 (2008).

²⁹B. R. Maddox, H. S. Park, B. A. Remington, N. Izumi, S. Chen, C. Chen, G. Kimminau, Z. Ali, M. J. Haugh, and Q. Ma, *Rev. Sci. Instrum.* **82**, 023111 (2011).

³⁰H. Chen, A. J. Link, R. van Maren, P. K. Patel, R. Shepherd, S. C. Wilks, and P. Beiersdorfer, *Rev. Sci. Instrum.* **79**, 10E533 (2008).

³¹J. D. Huba, *NRL Plasma Formulary* (Naval Research Laboratory, Washington, DC, 2011).

³²P. M. Nilson, W. Theobald, J. F. Myatt, C. Stoeckl, M. Storm, J. D. Zuegel, R. Betti, D. D. Meyerhofer, and T. C. Sangster, *Phys. Rev. E* **79**, 016406 (2009).

³³J. F. Seely, G. E. Holland, L. T. Hudson, C. I. Szabo, A. Henins, H.-S. Park, P. K. Patel, R. Tommasini, and J. M. Laming, *High Energy Density Phys.* **3**, 263 (2007).